8-2021

Simulation of the Frequency Split of the Fundamental Air Cavity Mode of a Loaded and Rolling Tire by Using Steady-State Transport Analysis

Won Hong Choi
Purdue University, choi124@purdue.edu

J Stuart Bolton
Purdue University, bolton@purdue.edu

Washington, DC, United States
Inter-Noise 2021
2021 August 1-5

SIMULATION OF THE FREQUENCY SPLIT OF THE FUNDAMENTAL AIR CAVITY MODE OF A LOADED AND ROLLING TIRE BY USING STEADY-STATE TRANSPORT ANALYSIS

Won Hong Choi, J. Stuart Bolton
Ray W. Herrick Laboratories, Purdue University

SCHOOL OF MECHANICAL ENGINEERING
AUGUST 3, 2021
Presentation available at: https://docs.lib.purdue.edu/herrick/

Content

1. Introduction
2. Steady-state transport analysis
3. Simulation results
4. Conclusion

Introduction

Background (1/3)

- Tire/road noise can be a dominant source of cabin and pass-by noise for Electric Vehicles
- The air-cavity mode is known to be a significant source of in-cabin vehicle noise, especially at frequencies near 200 Hz

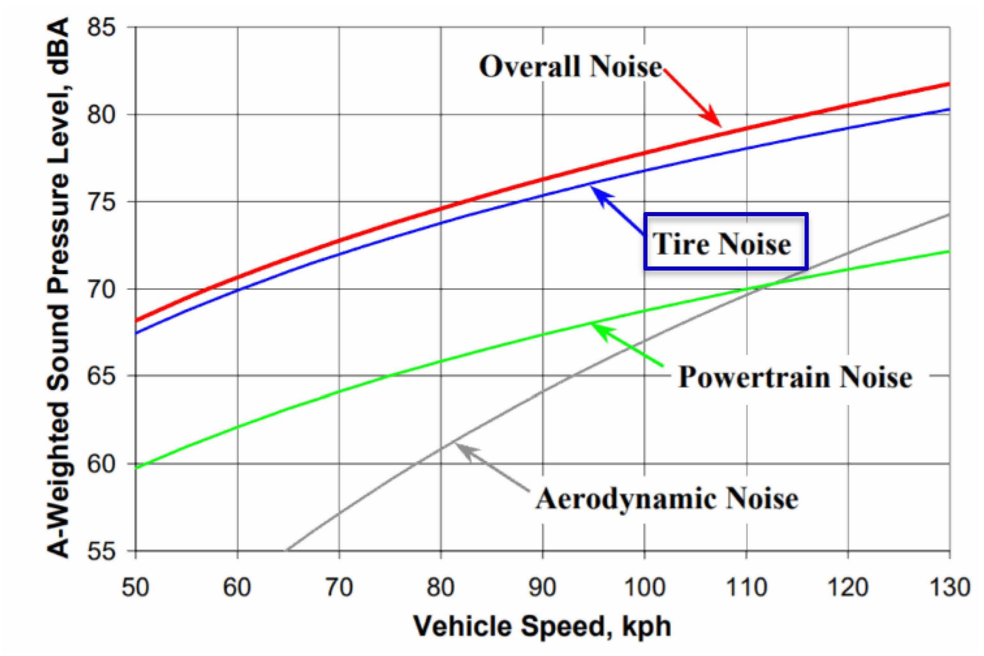

Dominance of tire/road noise, Purdue & U. of Central Florida [1]

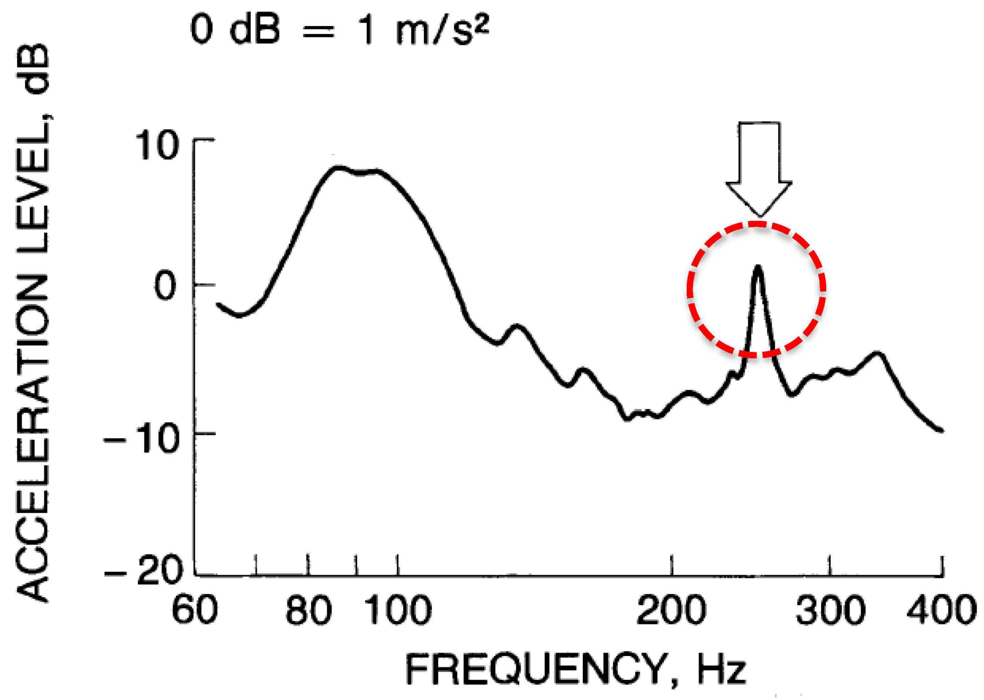

Observation of tire cavity mode, Sakata and *et al*. [2]

Background (2/3)

- This mode splits into two, a fore-aft and a vertical mode, when a tire is deformed by contact with the road, since geometrical symmetry is lost – this effect is referred to as a ‘frequency split’
- Higher level of interior noise & dynamic forces at the hub can occur if the two peaks are close to tire’s structural modes

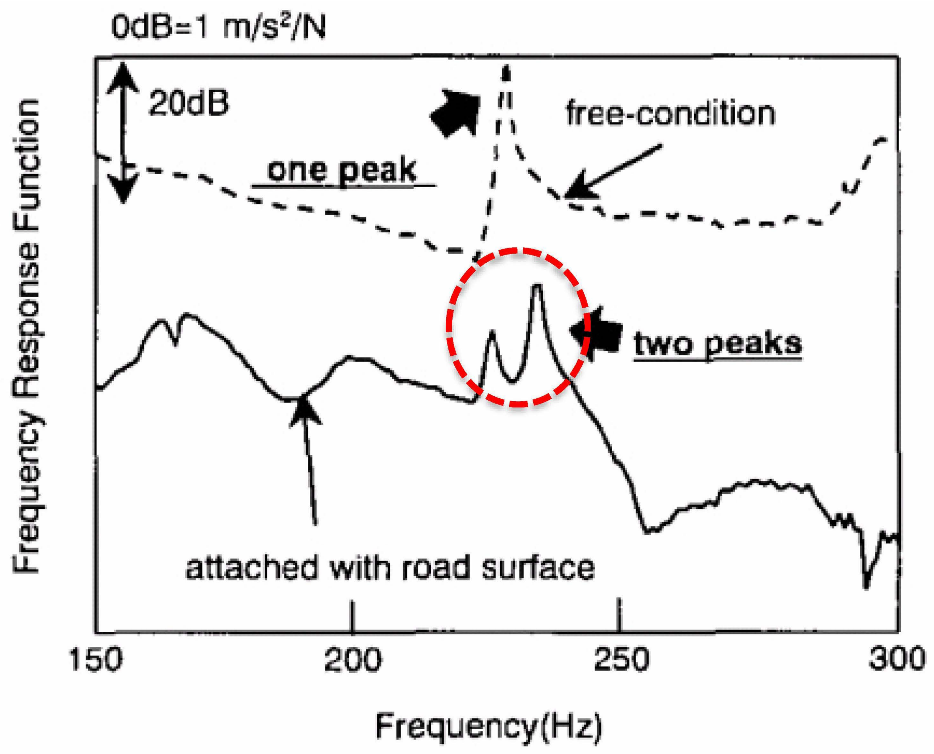

Split in air-cavity mode, Yamauchi and Akiyoshi [3]

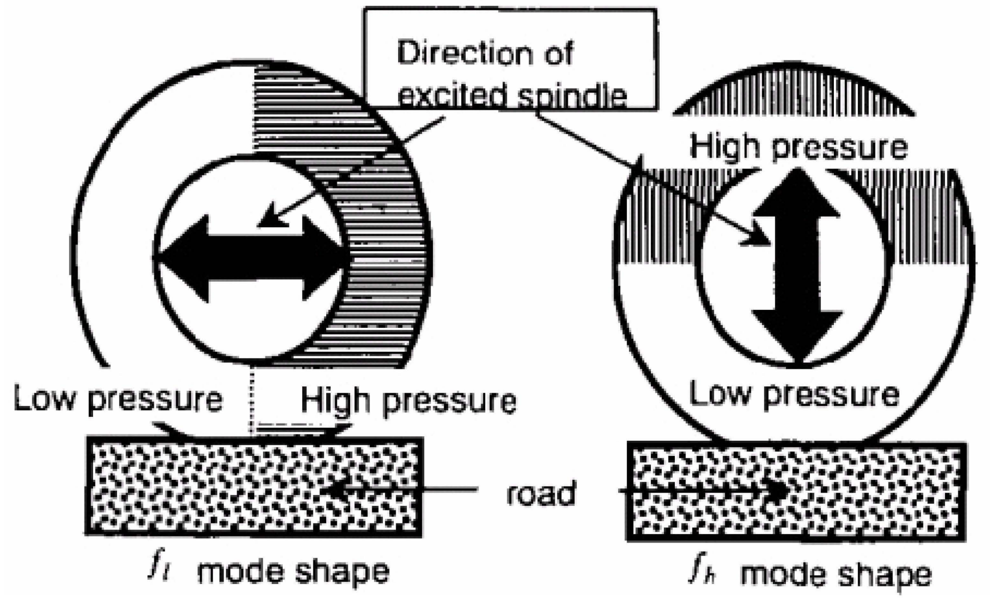

Two acoustic modes for loaded tire [3]

Introduction

Background (3/3)

- Tire rotation expands the frequency split owing to the Doppler effect which causes a difference in phase speeds in of acoustic wave propagation in the forward and backward circumferential directions within the tire cavity
- Structural modes also split and shift owing to the Doppler effect [6], broadening the frequency range of acoustic/structural interaction

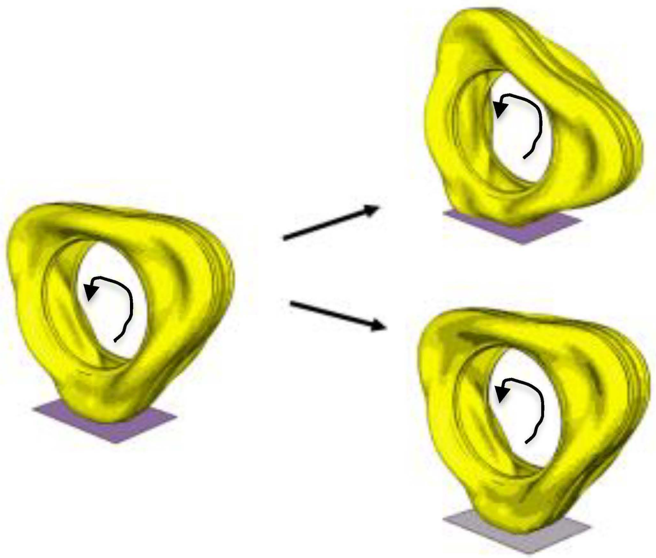

Split in structural mode for rolling tire, Abaqus [4]

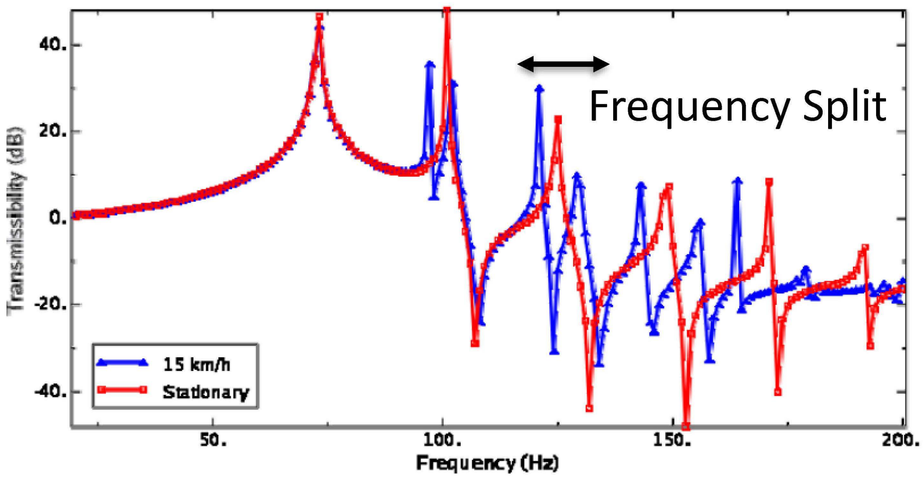

Split in forces at the hub for rolling tire, Abaqus [4]

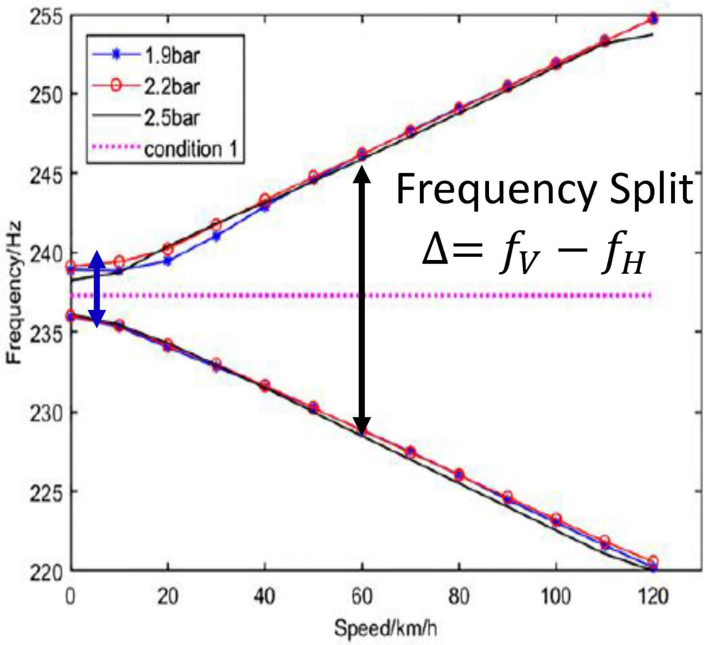

Split in acoustic mode for rolling tire, Yuting [5]

Introduction

Objective

- Observe ‘Frequency-split’ of fundamental cavity mode for deformed tires, including rotation effects, in simulation prior to performing experiments for two modeled tires
- The influence of rotation on forces at the hub will be investigated

No.	Rim	Width	Aspect ratio	Inflation	Rated load	Remark
R18	18 inch	235 mm	50	35 psi	5496 N	Max. at 60km/h
R20	20 inch	265 mm	35	35 psi	4812 N	Max. at 60km/h

Stage 1. Test on static tires

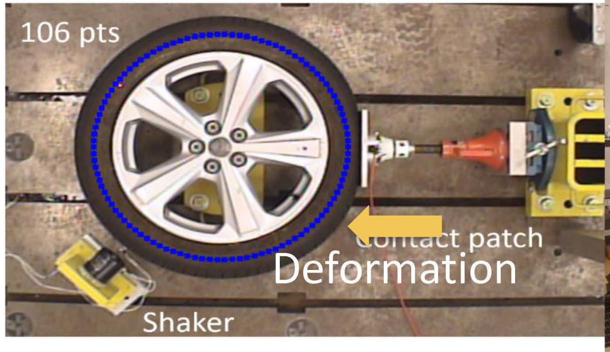

Shaker at 135° from contact patch

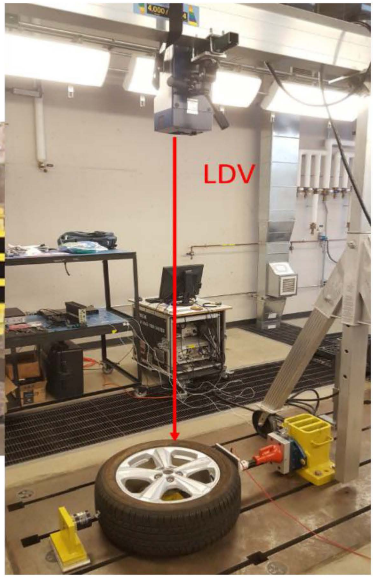

Transition

Stage 2.
Test on rolling tires

Steady-state transport analysis

- Steady-State Transport Analysis (SSTA) makes it possible to simulate rolling tires without implementing time-based transient analysis, using frequency-based, harmonic analysis
- Angular velocity (ω) can be defined by making the transformation from a local axis to a global coordinate system
- Solutions converge faster in the acoustic domain as a result of modeling material flow along streamlines inside the acoustic mesh under rotation, while the structural mesh remains a conventional Lagrangian mesh

1. Symmetric Model Generation (SMG)

- Treadband (2D shell)
- Sidewall (2D shell)
- Air (3D solid)

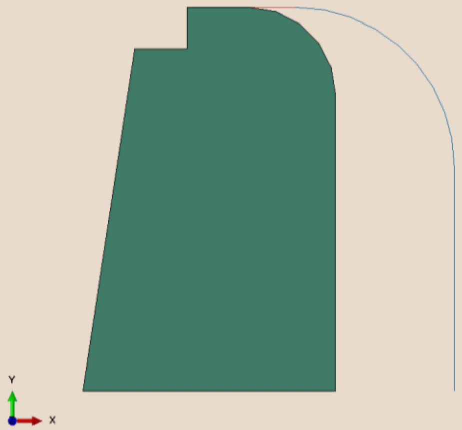

2. Static Analysis

- Inflation analysis
- Foot print analysis

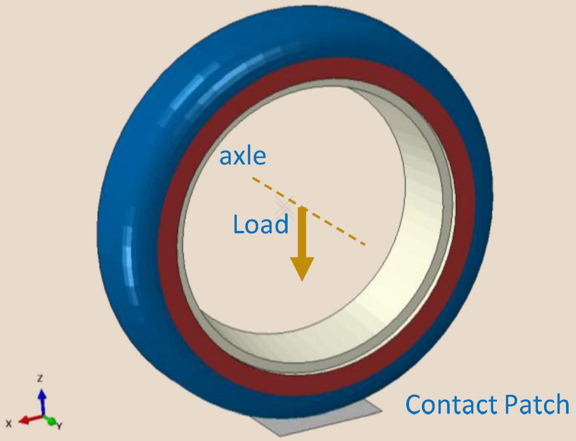

3. Steady State Transport (SST)

- Modal analysis
- Harmonic analysis for rolling tire

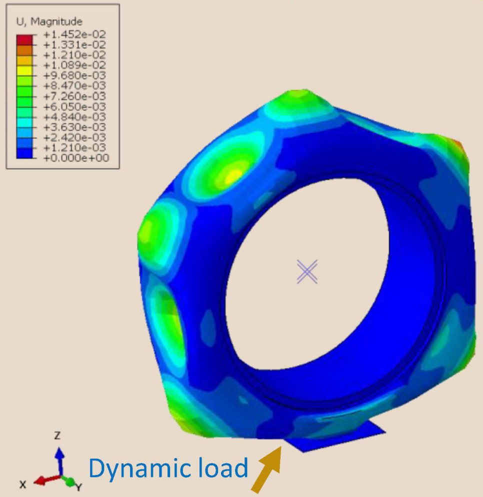

Finite element model

FE Model

- Quarter-symmetric model was created to represent the cross-sectional geometry
- Rim and contact patch were considered to be rigid bodies here

Parameters	R18	R20
Rim [inch]	18	20
Width [mm]	235	265
Aspect ratio	50	35
Mass [kg]	12.7	13.2
Stiffness [N/mm]	306	349
Inflation [MPa]	0.24	0.24
Rated load [N]	5496	4812

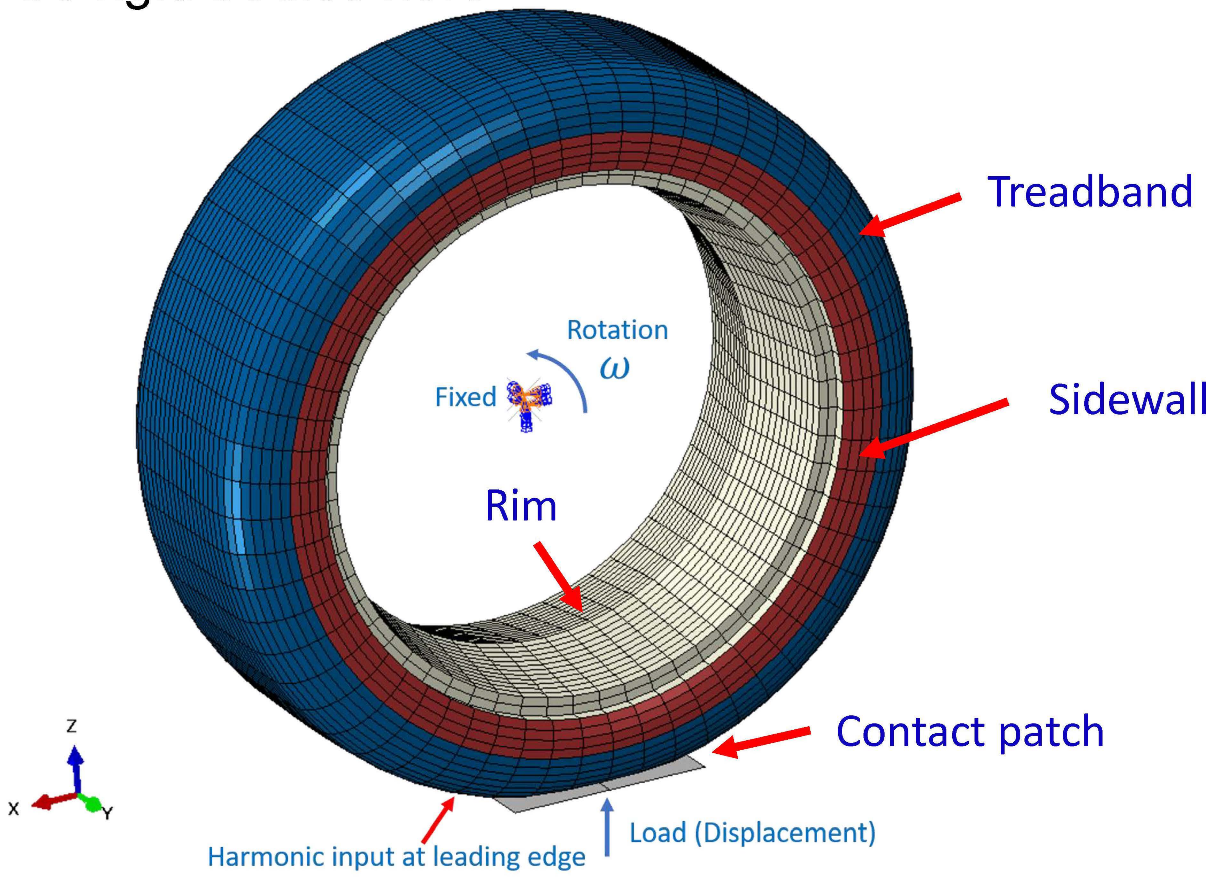

Finite element model

Material properties

- An equivalent constant thickness and input properties concerning reinforcement belts and carcass, such as alignment, surface area, and spacing, were also embedded in shell elements
- Air properties were determined for an inflated tire at room temperature, 28℃ , similar to the test environment.

<Tire structure>

Parameters	Part	R18	R20
Thickness [mm]	Treadband	12	8
	Sidewall	6	6
Density [kg/m^3]	Treadband	1520	1690
	Sidewall	1013	1120
Young's modulus (E) [MPa]	Treadband	150	150
	Sidewall	50	5
	Belt (2)	25,000	150,000
	Carcass (1)	900	900
Poisson's ratio (υ)	All	0.3	0.3

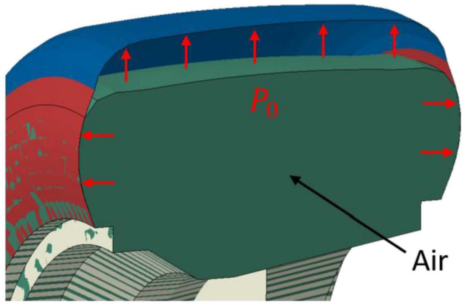

<Air>

Air density [kg/m^3]	4.3
Bulk modulus [MPa]	0.52

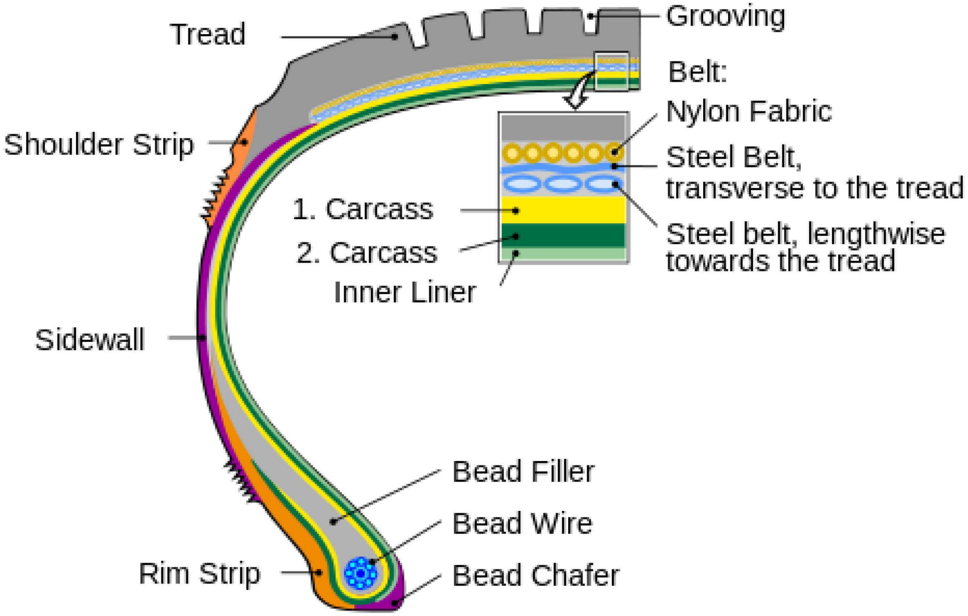

Tire composition, courtesy of Wikipedia

Analysis of simulation results

Mobility and Dispersion

- Mobility data can be obtained by "measuring" surface velocity (V) and input force (f) for the deformed tire for 106 points along sidewall, as for experimental results obtained by using Laser Doppler Vibrometer
- Wavenumber components (k_θ) can be identified by applying Discrete Fourier Transform to the mobility data spatially distributed along sidewall

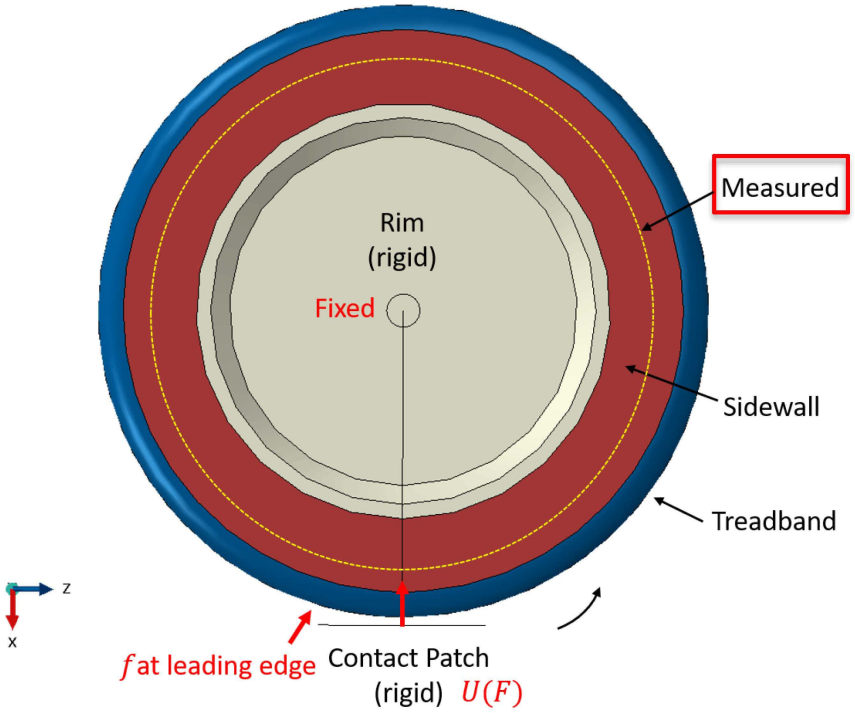

1. Inflation

↓

2. Deformation

↓

3. Modal analysis

↓

4. Harmonic analysis (static)

↓

5. Harmonic analysis (dynamic)

Simulation results

Verification in the absence of rotation for non-deformed tire, Mobility, R18

- The results confirm that the two patterns are in a good agreement, especially near 200 Hz, close to the acoustic cavity mode
- The pattern indicates the occurrence of natural structural modes at various frequencies, the order of the mode increasing with frequency

(a) Simulation

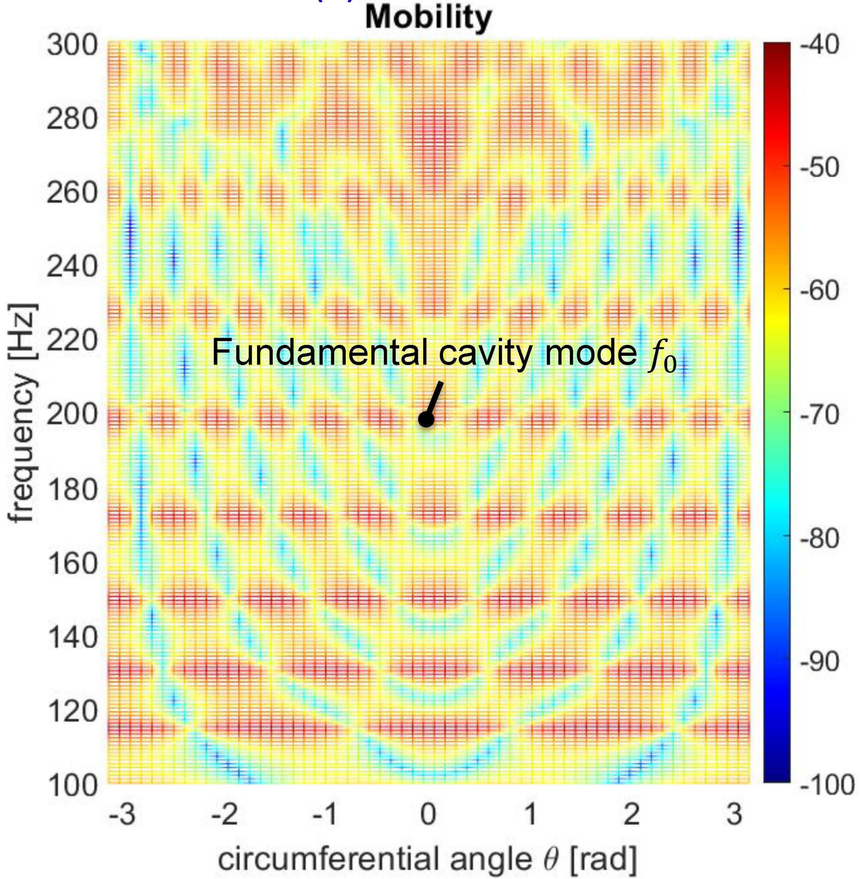

(b) Test

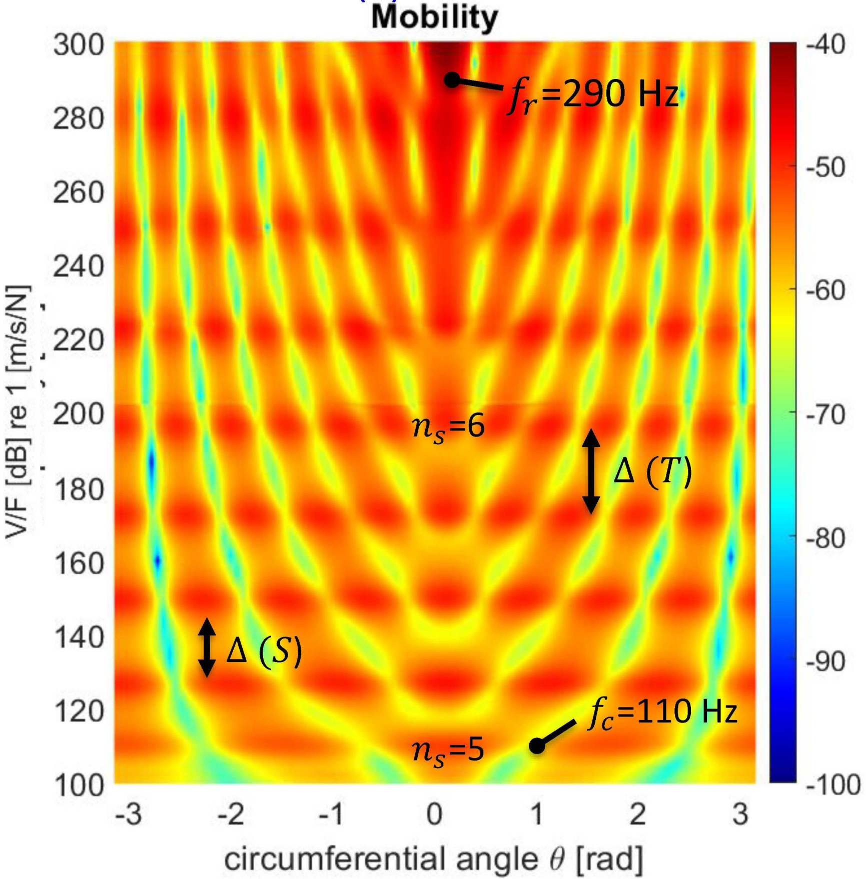

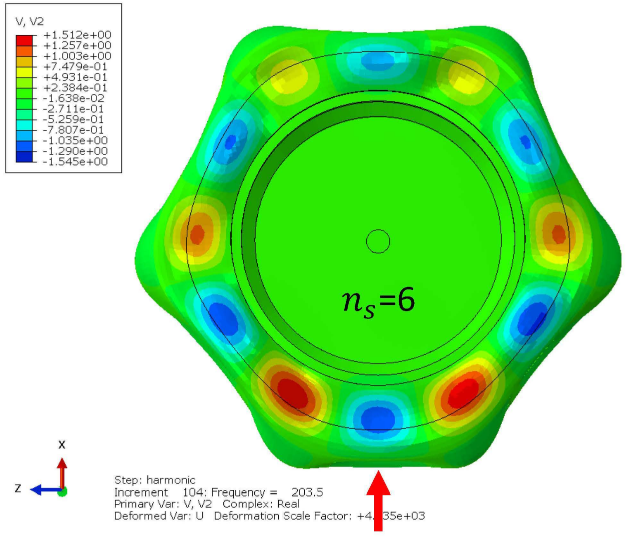

f_0 : fundamental cavity mode
f_r : ring frequency
f_c : cut-on frequency
n_s : mode number on sidewall
$\Delta(S)$: mode interval on sidewall
$\Delta(T)$: mode interval on tread

Simulation results

Verification in the absence of rotation for non-deformed tire, Dispersion, R18

- All of the structural modes are placed at equivalent positions with the same phase speed, and also the acoustic cavity mode appears at the same frequency and wavenumber in both cases

(a) Simulation

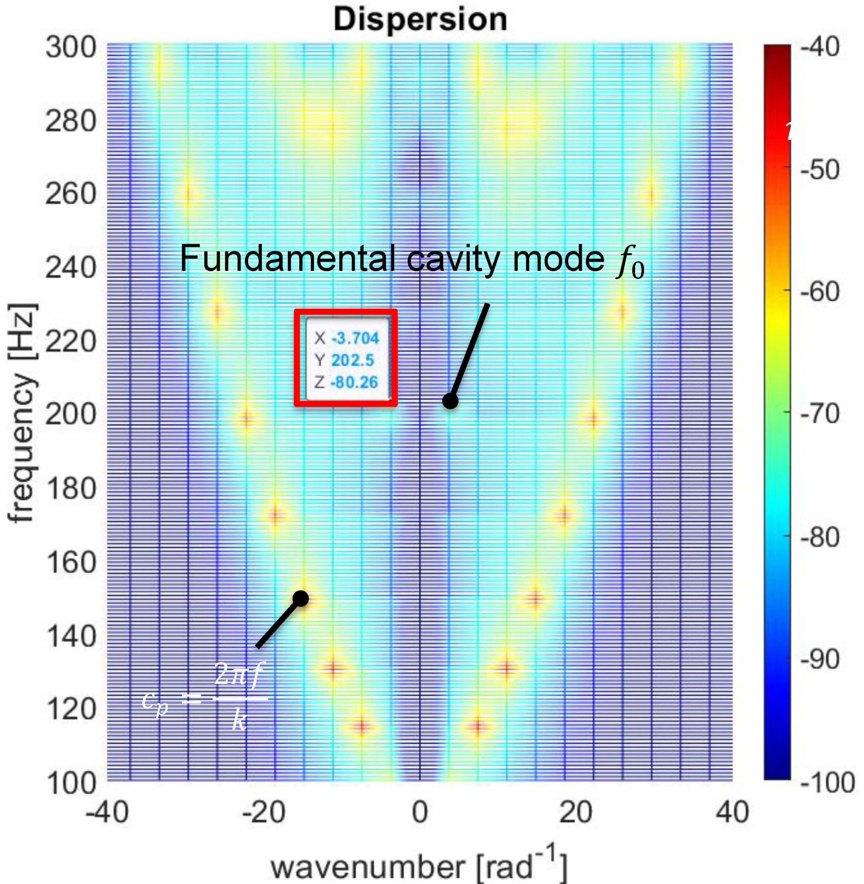

(b) Test

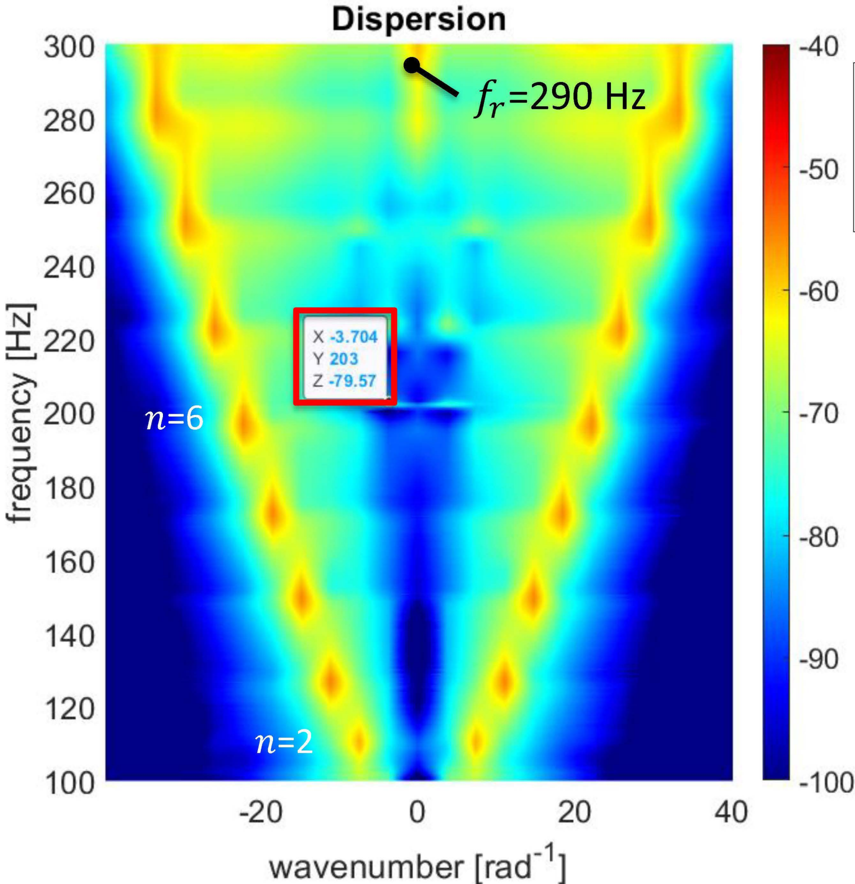

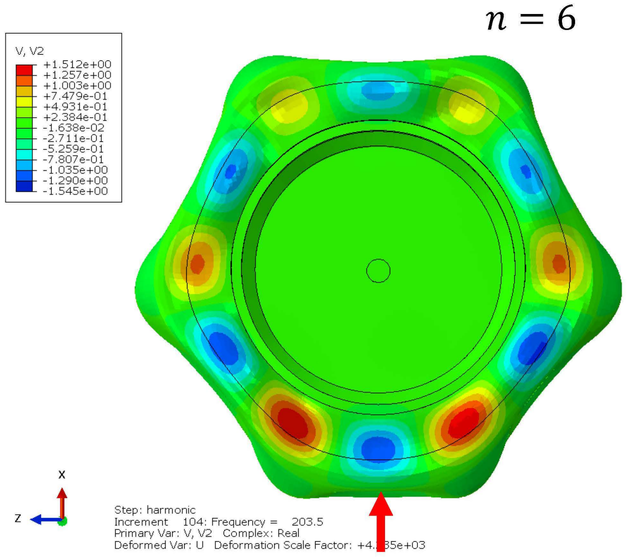

n : mode number on tread

c_p : phase speed of wave

Simulation results

Verification in the absence of rotation for non-deformed tire, Mobility, R20

- Good agreement between the two results in terms of structural patterns and the appearance of the fundamental cavity mode near 200 Hz

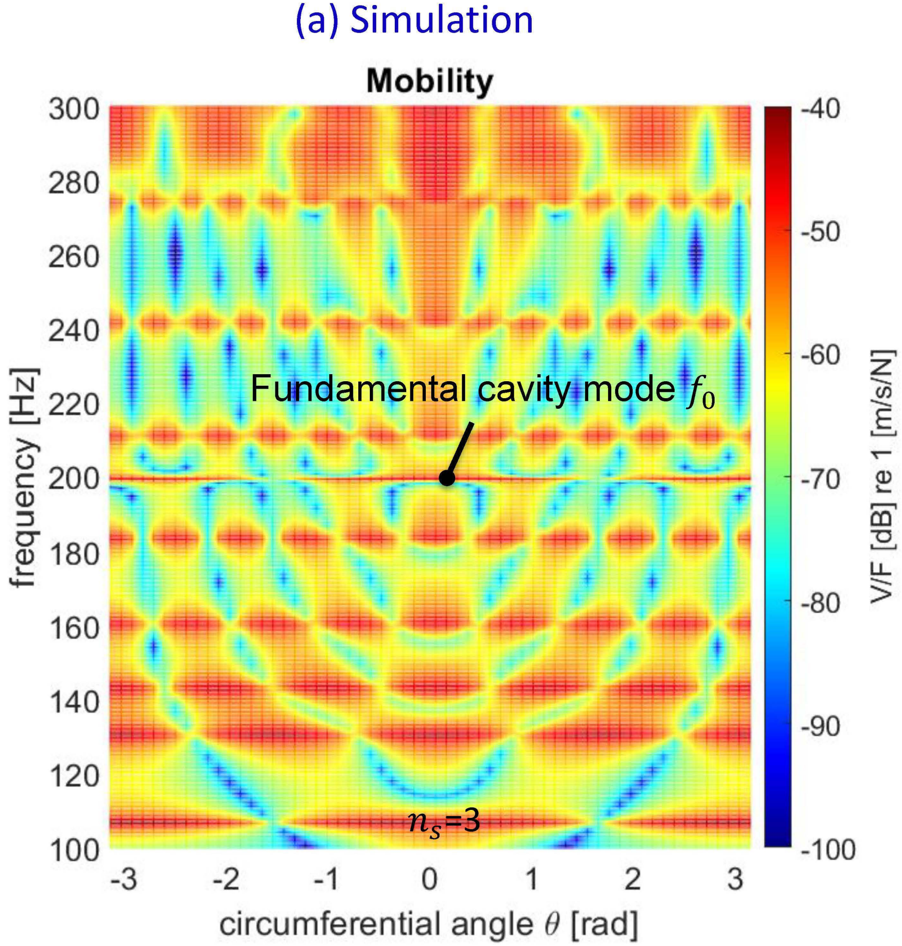

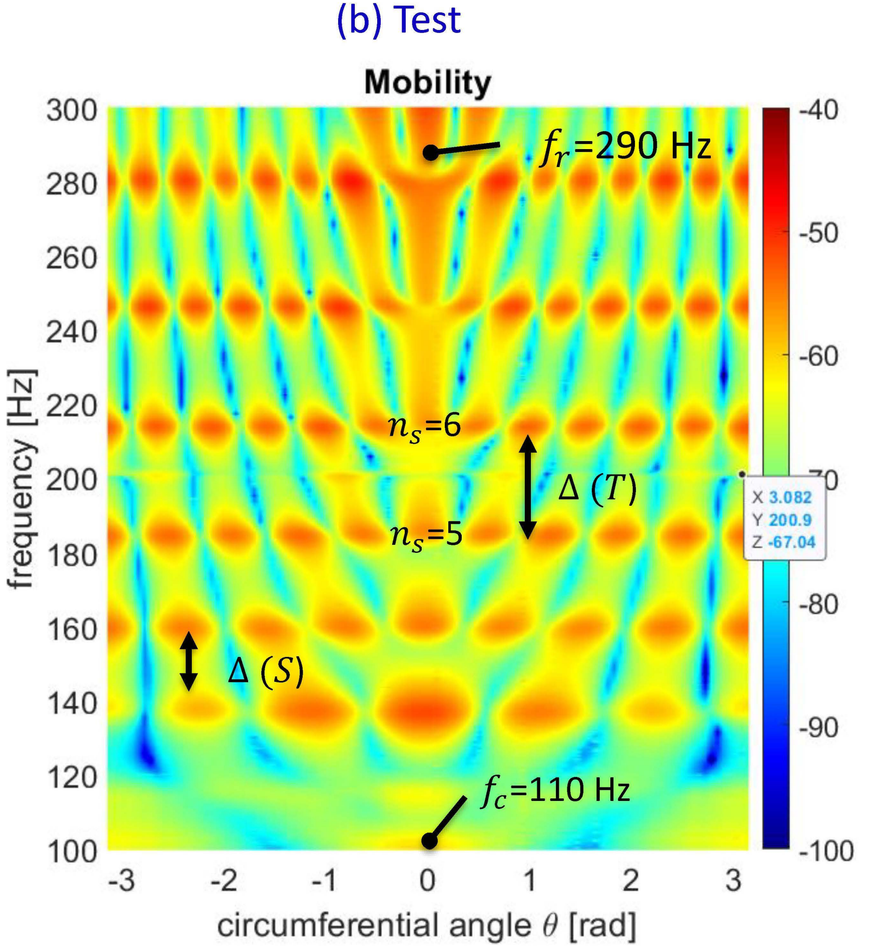

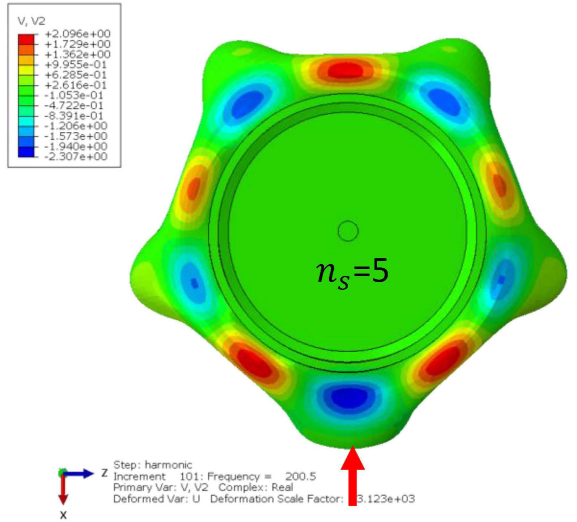

f_0 : fundamental cavity mode
f_r : ring frequency
f_c : cut-on frequency
n_s : mode number on sidewall
$\Delta(S)$: mode interval on sidewall
$\Delta(T)$: mode interval on tread

Simulation results

Verification in the absence of rotation for non-deformed tire, Dispersion, R20

- Demonstrates the reliability of the simulation in reproducing wave propagation from 100 Hz to 300 Hz for statically coupled tires.

(a) Simulation

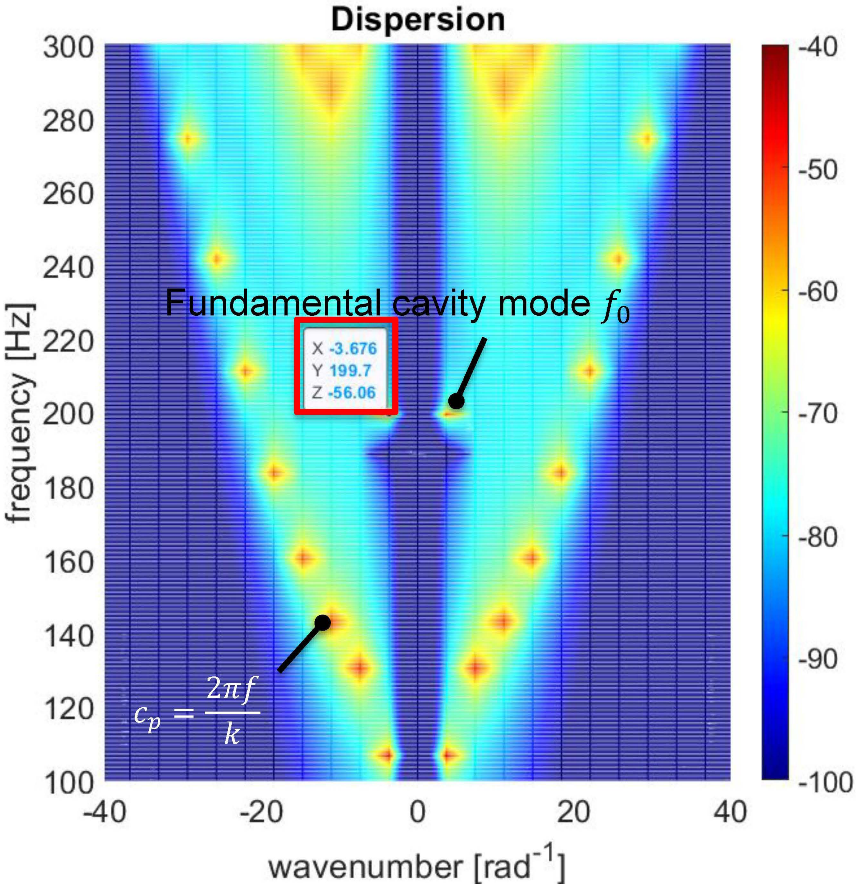

(b) Test

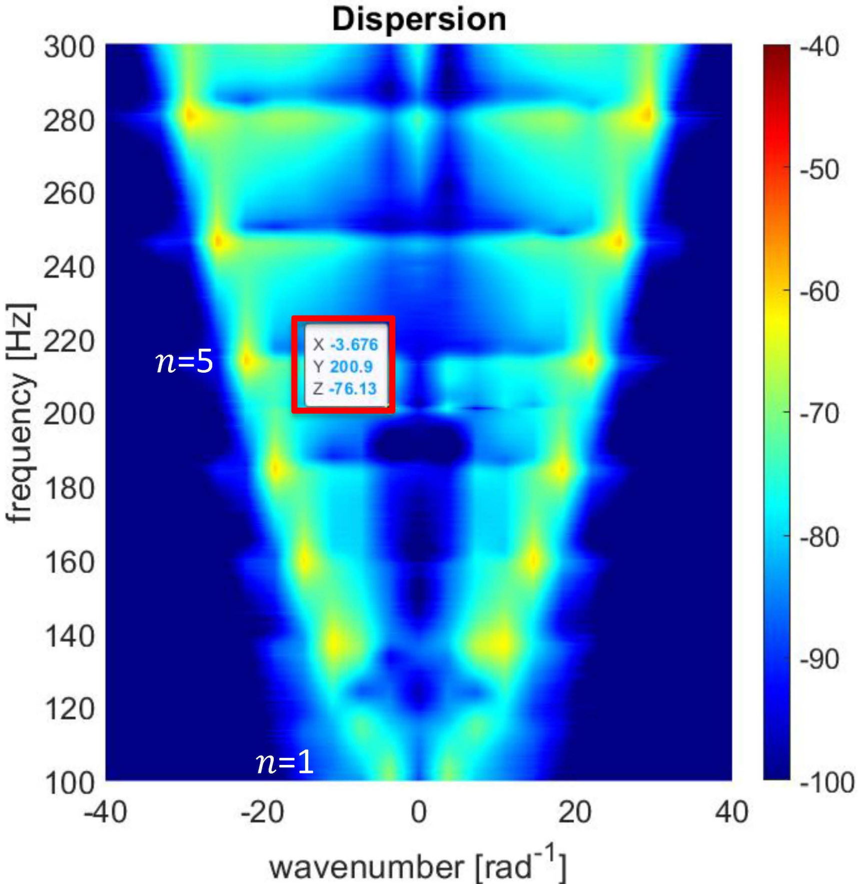

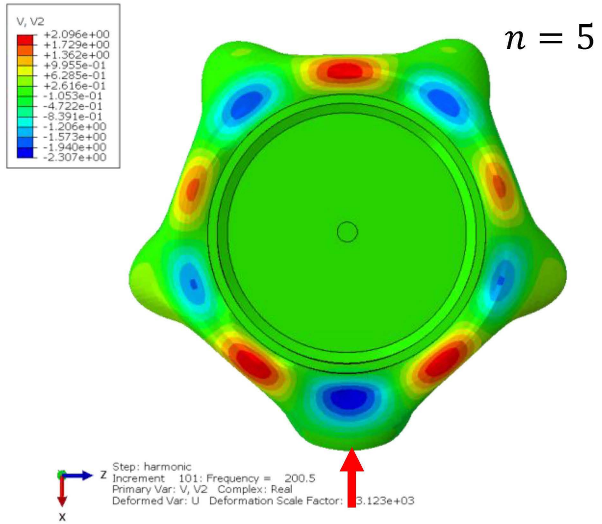

n : mode number on tread

c_p : phase speed of wave

Simulation results

The influence of rotation on the mobility relation for deformed tire, R18

- The frequency split increased from 7.1 Hz to 16.6 Hz when the speed increased from 0 km/h to 60 km/h
- A sub-structural mode at 140 Hz, for instance, can be seen in the right figure, indicating that structural modes are also split due to the rotation effect

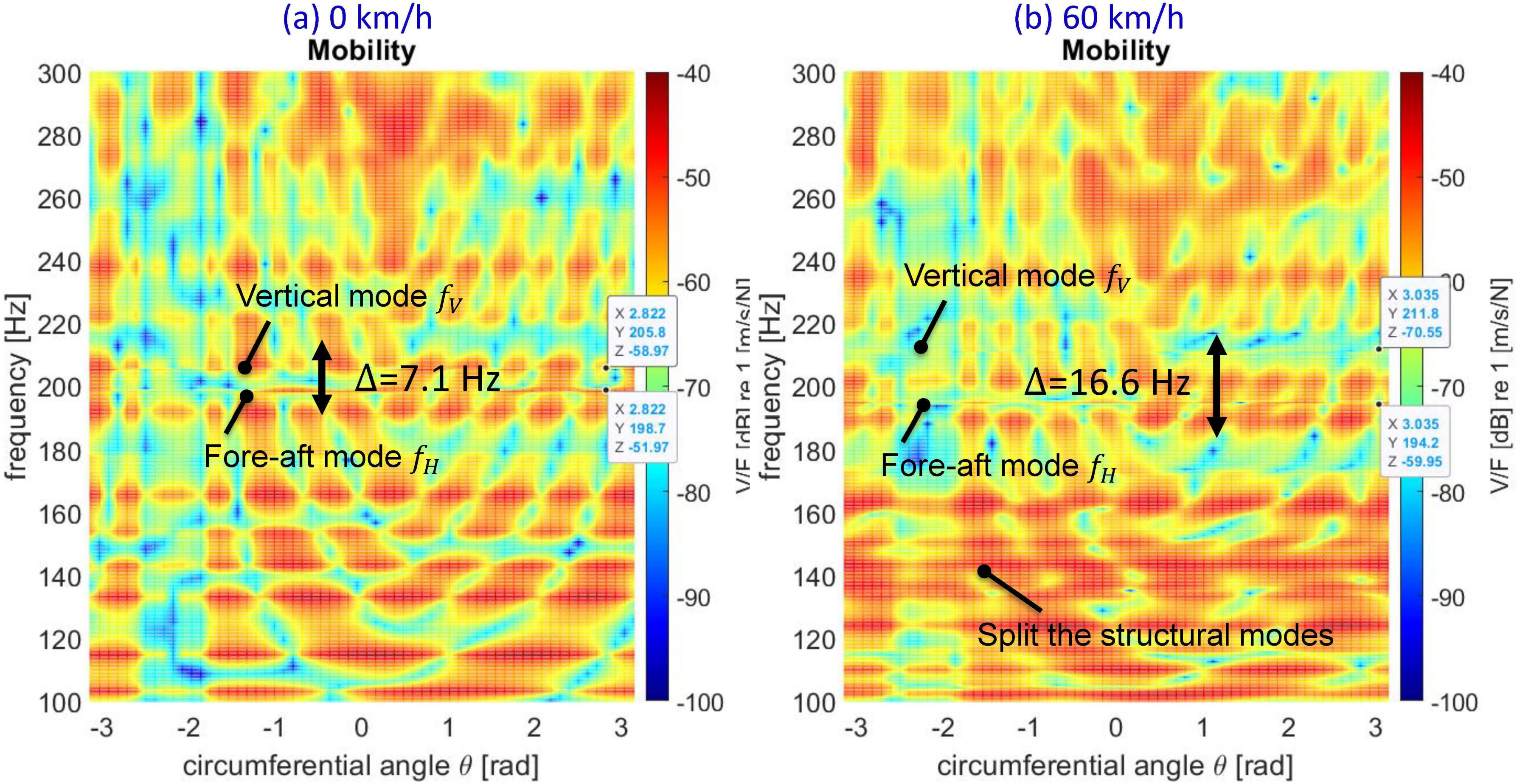

Δ: frequency split in acoustic mode

Simulation results

The influence of rotation on the dispersion relation for deformed tire, R18

- A tilting effect can be seen in the dispersion curves, caused by the different phase speeds of the positive and negative-going structural waves in the circumferential direction.

(a) 0 km/h

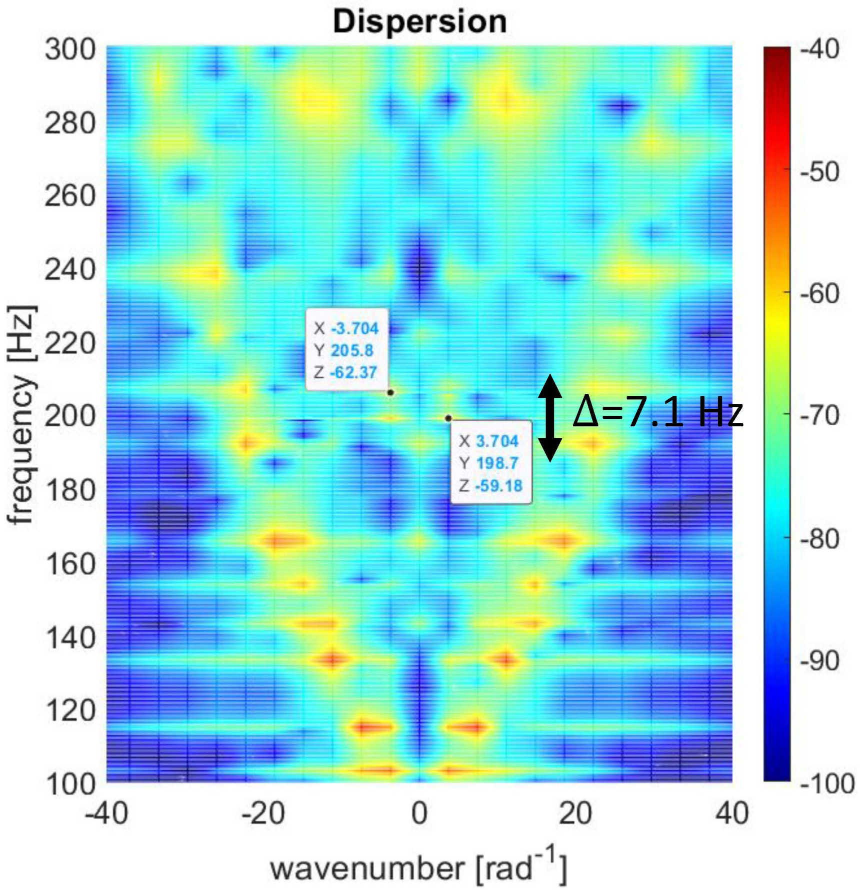

(b) 60 km/h

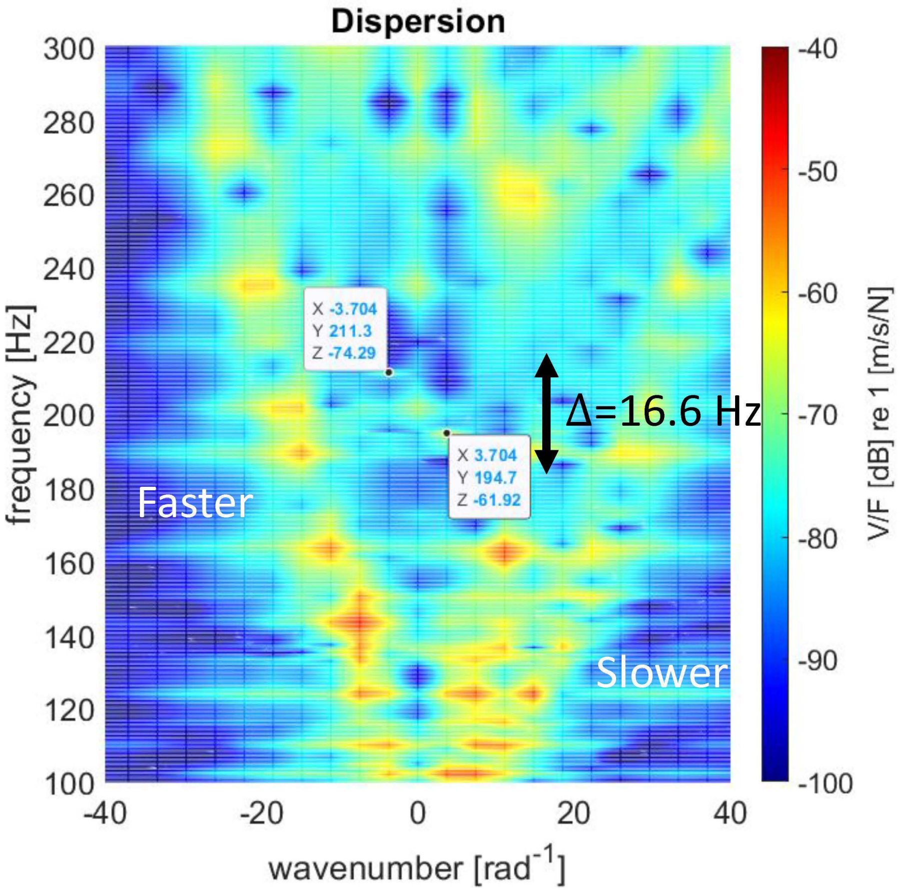

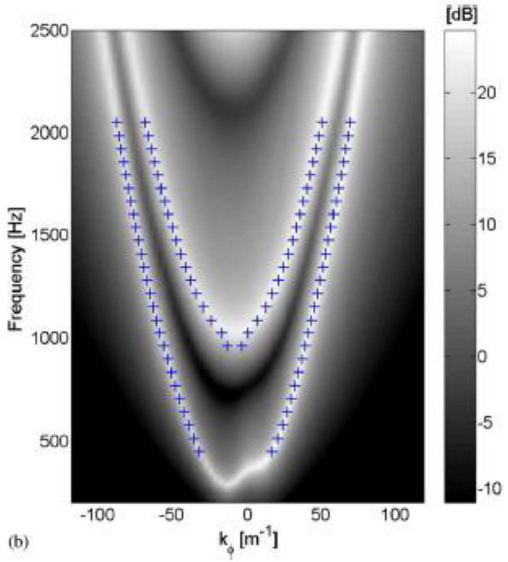

Tilting effect in analytical tire model, Y.J., Kim [6]

Δ: frequency split in acoustic mode

The influence of rotation on the acoustic pressure for deformed tire, R18

- Phase speed of fore-aft mode is slower, decreasing natural frequency at 60 km/h
- Phase speed of vertical mode is faster, increasing natural frequency at 60 km/h

Fore-aft mode, f_H

Vertical mode, f_V

0 km/h

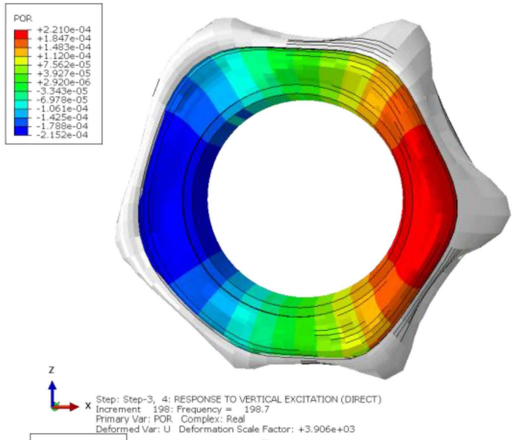

198.7 HZ

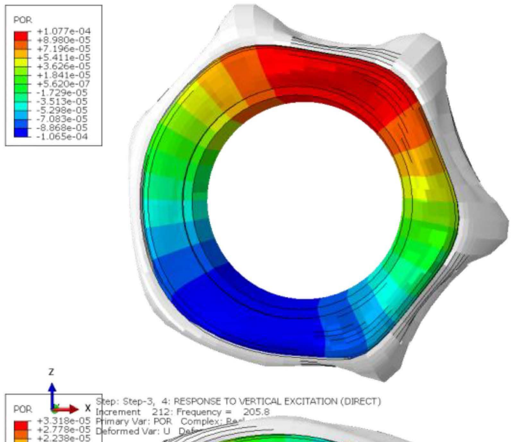

205.8 HZ

60 km/h

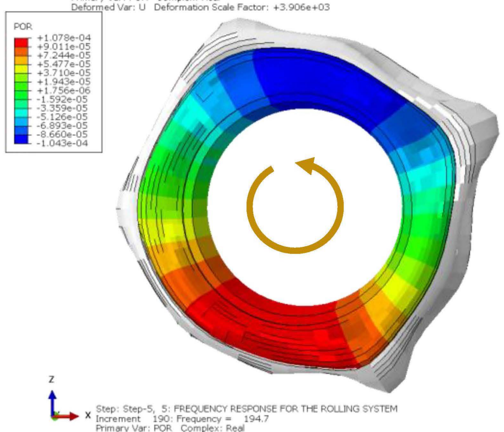

194.7 HZ

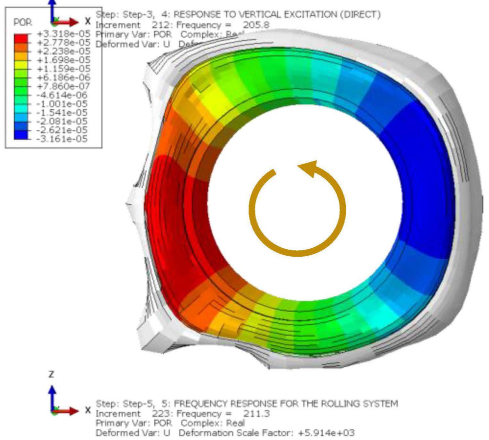

211.3 HZ

The influence of rotation on the mobility relation for deformed tire, R20

- The frequency split increased from 4.6 Hz to 16.6 Hz when the speed increased from 0 km/h to 60 km/h, accompanied by splitting of structural modes

(a) 0 km/h

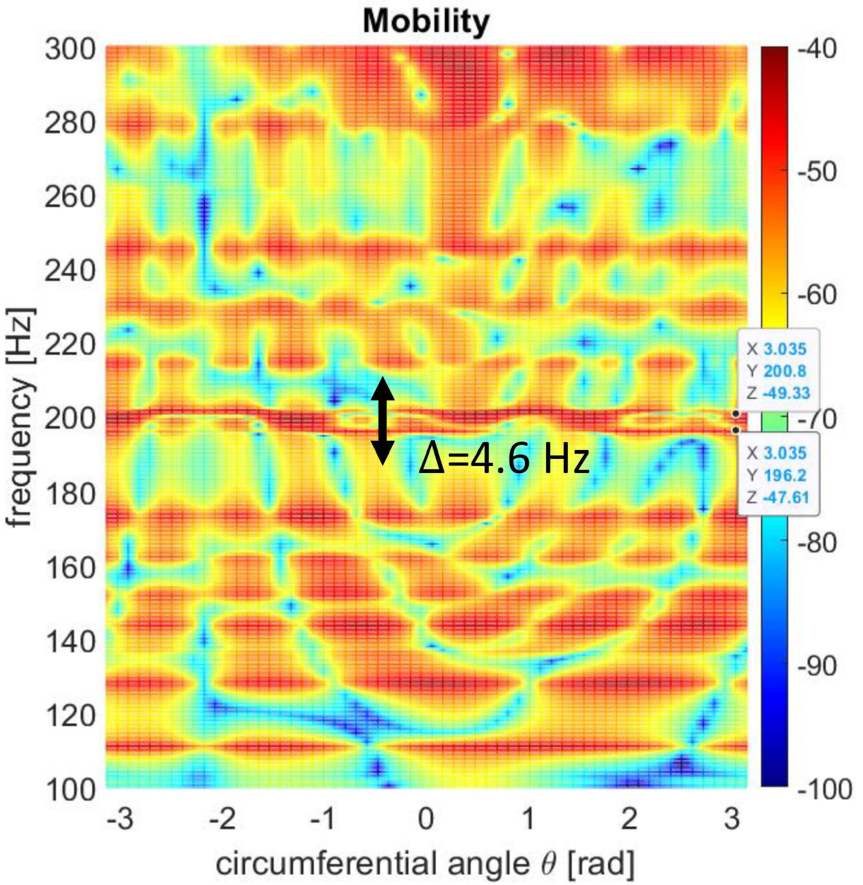

(b) 60 km/h

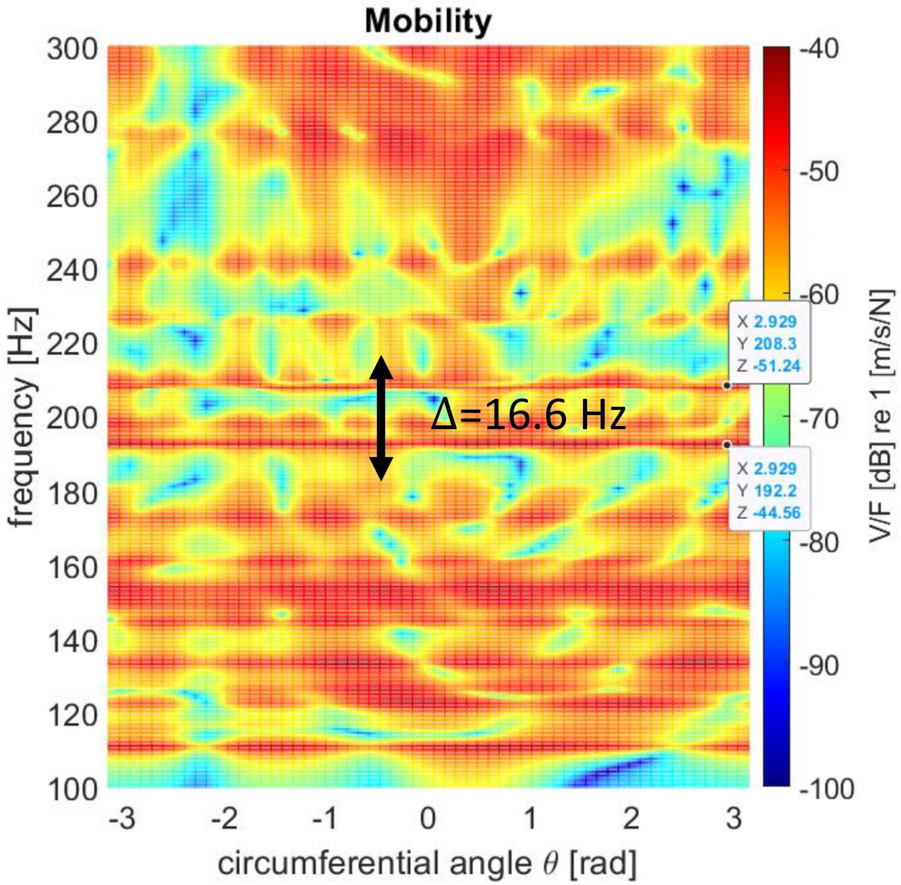

Δ: frequency split in acoustic mode

Simulation results

The influence of rotation on the dispersion relation for deformed tire, R20

- The tilting phenomenon in the right curve shown can also be observed, owing to the different phase speeds in the two wave propagation directions

(a) 0 km/h

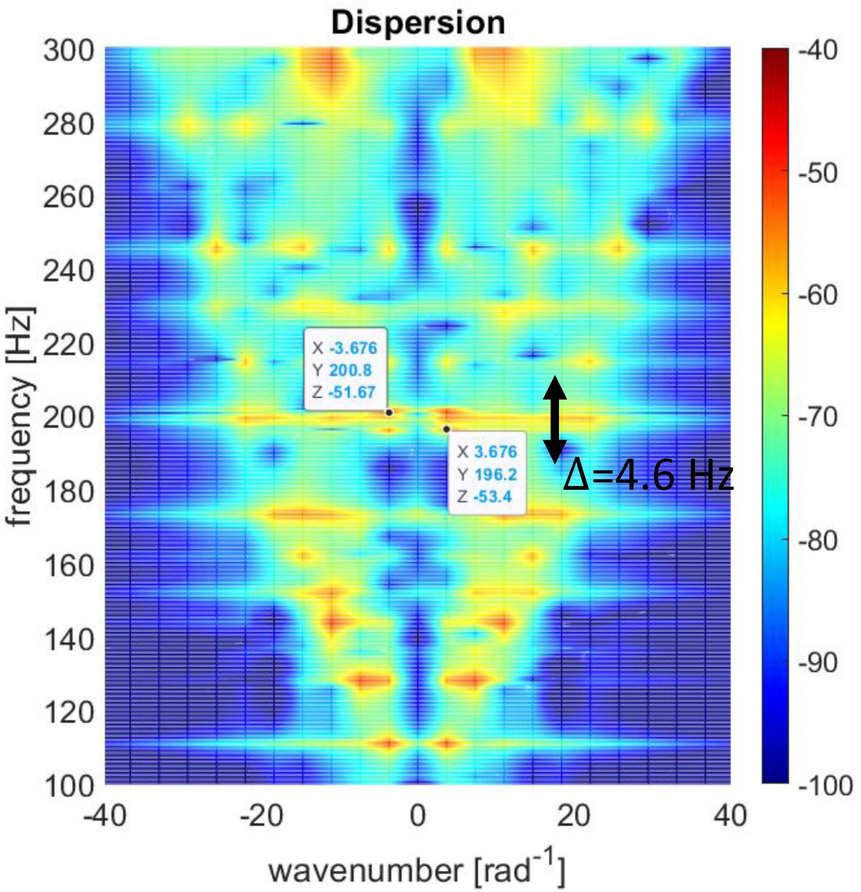

(b) 60 km/h

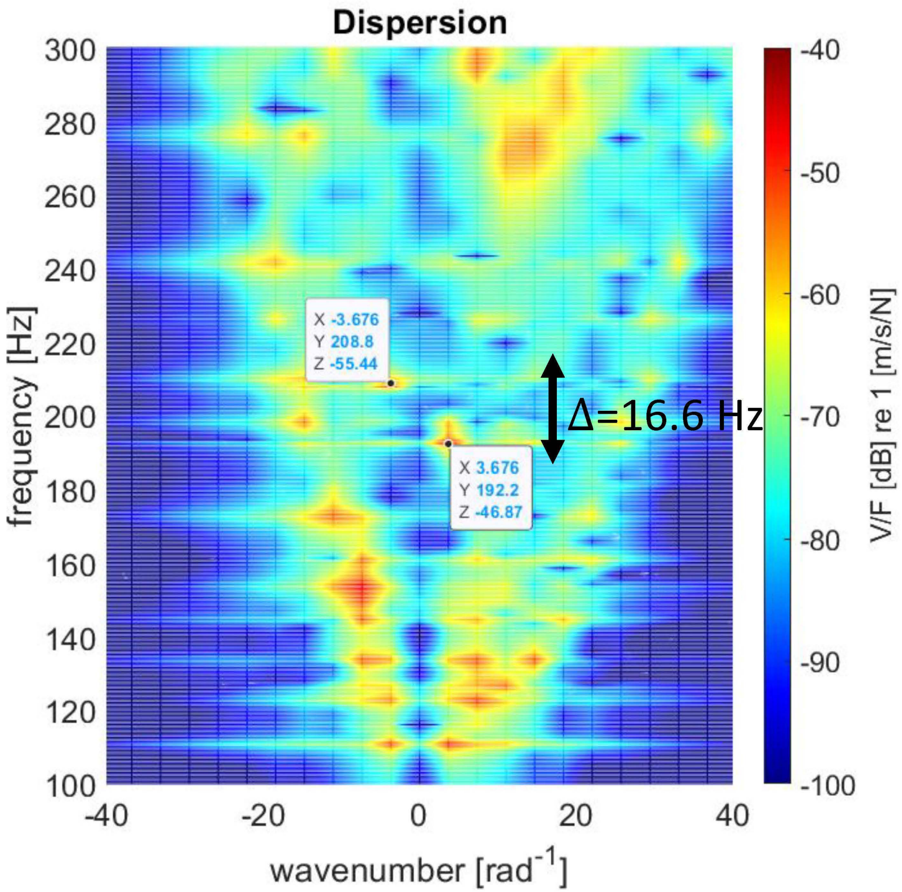

Δ: frequency split in acoustic mode

Simulation results

The influence of rotation on the acoustic pressure for deformed tire, R20

- Phase speed of fore-aft mode is slower, decreasing natural frequency at 60 km/h
- Phase speed of vertical mode is faster, increasing natural frequency at 60 km/h

Fore-aft mode, f_H

Vertical mode, f_V

0 km/h

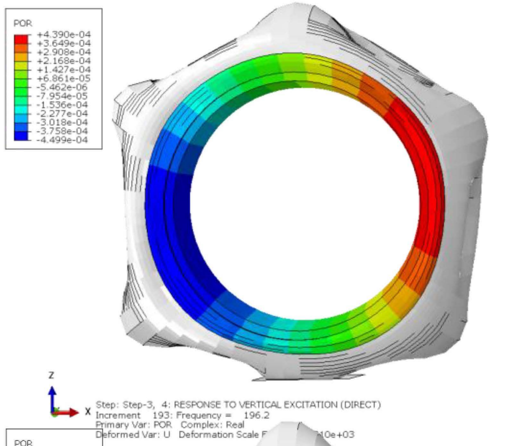

196.2 HZ

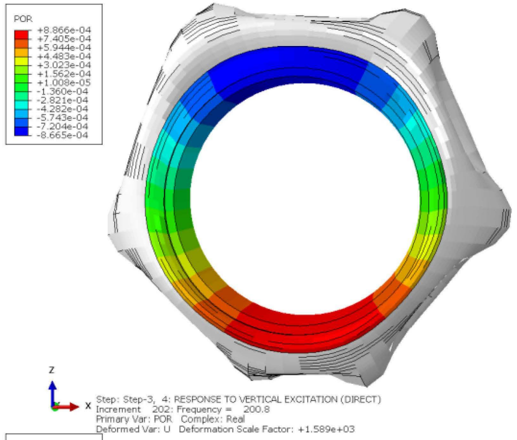

200.8 HZ

60 km/h

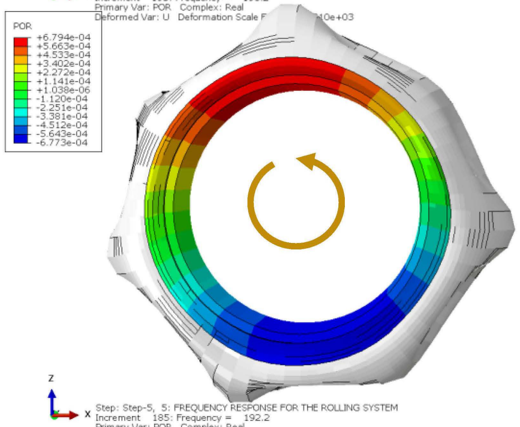

192.2 HZ

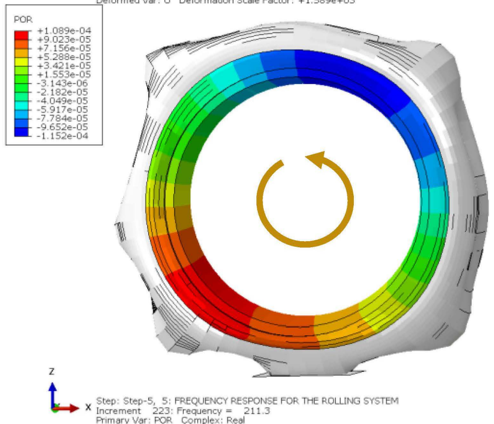

208.8 HZ

Simulation results

The influence of rotation on the frequency split for deformed tire, R18

- The split does not change significantly up to 20 km/h, and then it increases in proportion to the rotation speed, behavior which matches qualitative expectations

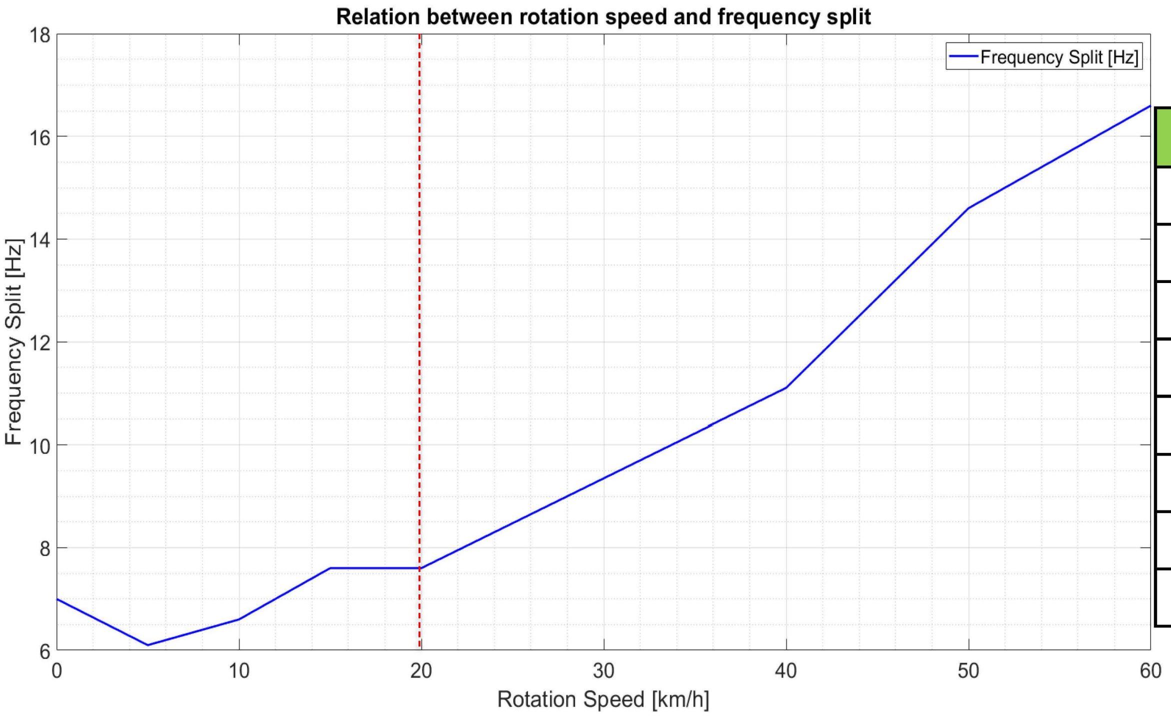

Rotation Speed	f_H [Hz]	f_V [Hz]	Δf [Hz]
0 km/h	198.7	205.8	7.1
5 km/h	199.2	205.3	6.1
10 km/h	199.2	205.8	6.6
15 km/h	198.7	206.3	7.6
20 km/h	199.2	206.8	7.6
40 km/h	197.2	208.3	11.1
50 km/h	194.7	209.3	14.6
60 km/h	194.7	211.3	16.6

Simulation results

The influence of rotation on the frequency split for deformed tire, R20

- The relation between the frequency split and rotation speed is almost linear, except at speeds lower than 20 km/h

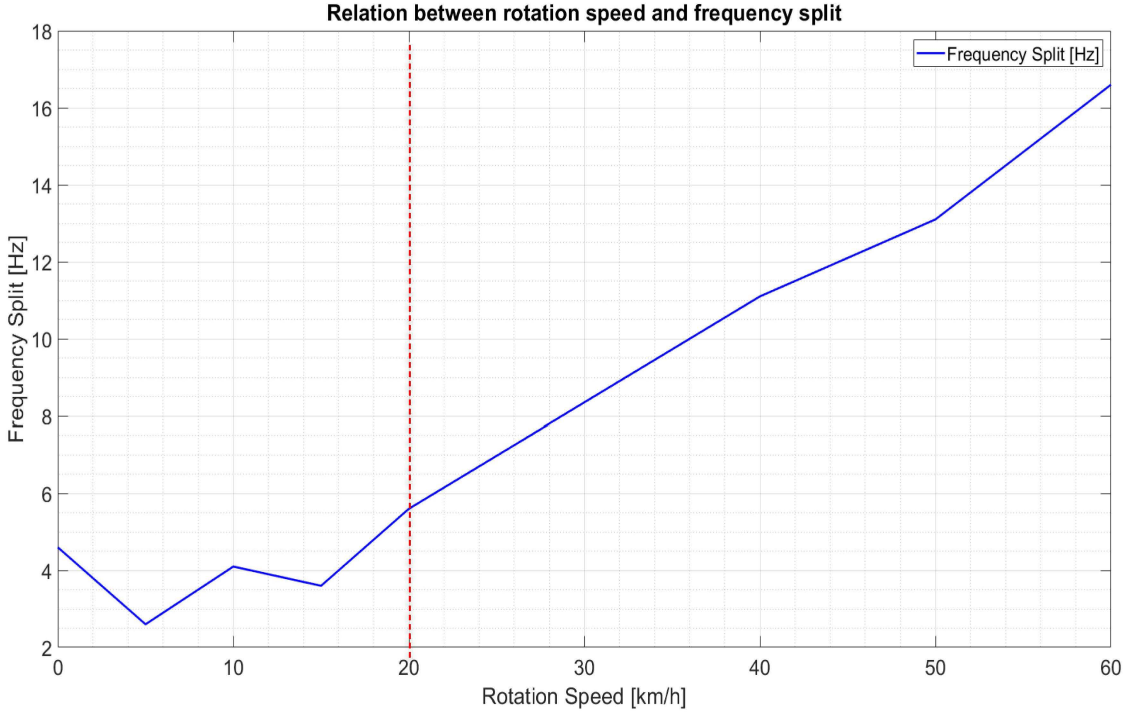

Rotation Speed	f_H [Hz]	f_V [Hz]	Δf [Hz]
0 km/h	196.2	200.8	4.6
5 km/h	199.2	201.8	2.6
10 km/h	198.7	202.8	4.1
15 km/h	199.2	202.8	3.6
20 km/h	197.2	202.8	5.6
40 km/h	194.7	205.8	11.1
50 km/h	193.7	206.8	13.1
60 km/h	192.2	208.8	16.6

Simulation results

The influence of rotation on forces at the hub for deformed tire, R18

- The force at the hub near 200 Hz is determined by an interaction between the air-cavity modes and the neighboring structural modes
- The peak is decreased in both the horizontal and vertical directions in the rotating case, which implies that the rotation not only affects the split in the acoustical mode, but also has an effect on the structural modes, which, in turn, affects the resultant force levels

(a) 0 km/h

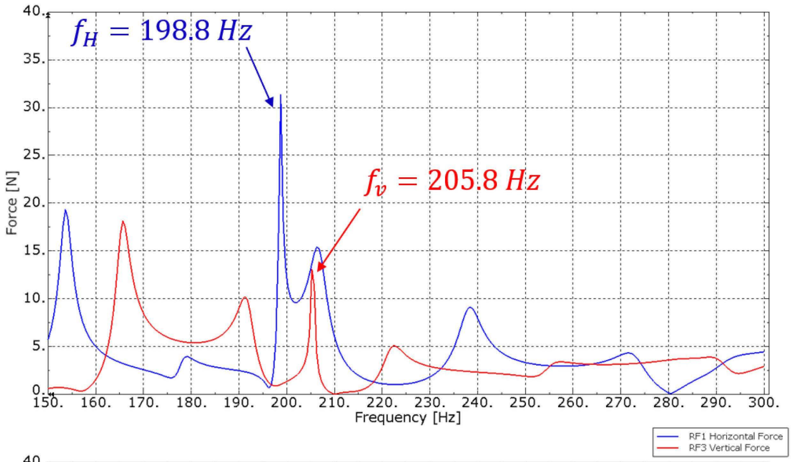

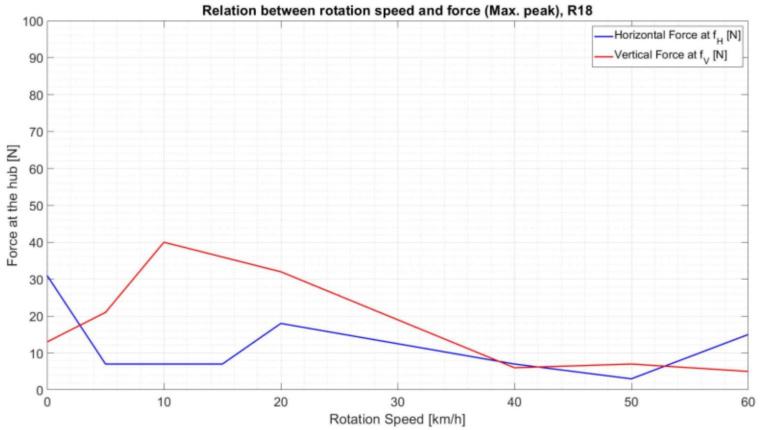

(b) 60 km/h

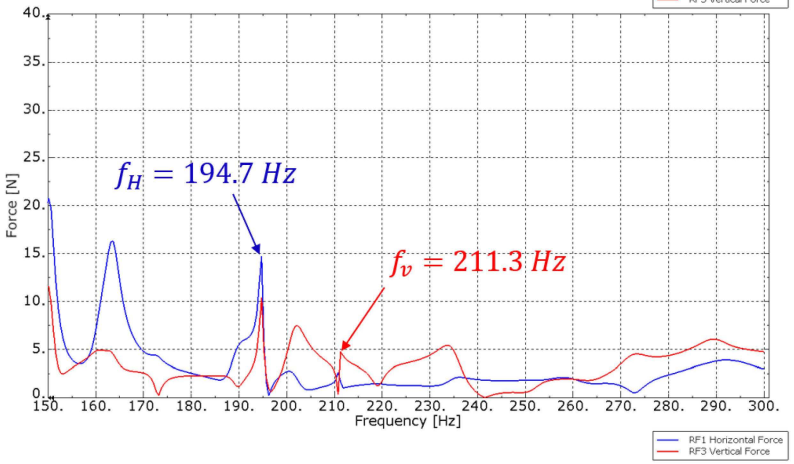

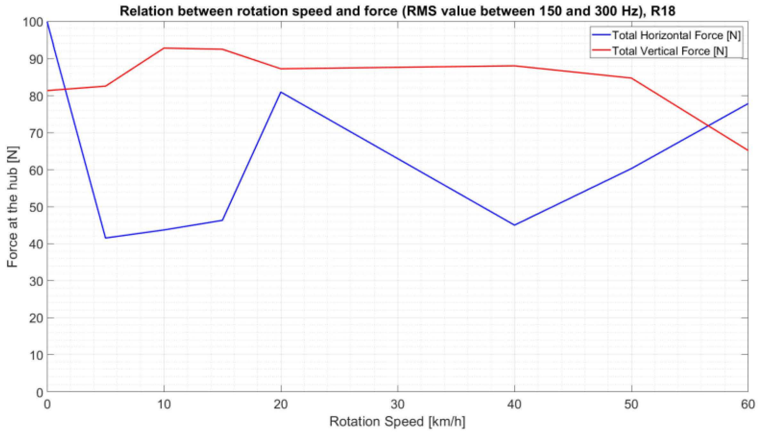

Simulation results

The influence of rotation on forces at the hub for deformed tire, R20

- The largest response in the vertical direction occurs at 0 km/h and it tends to decrease as speed increases, while, in contrast, the horizontal force is generally increasing with increasing speed, reaching a maximum at 60 km/h.

(a) 0 km/h

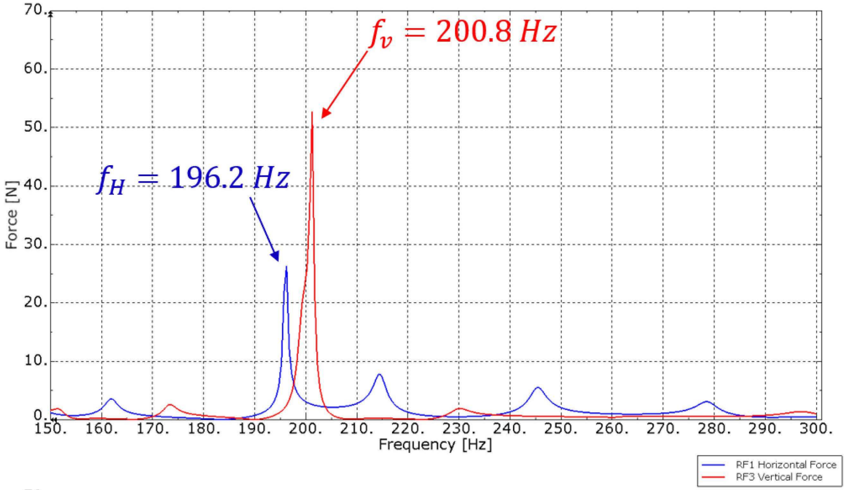

(b) 60 km/h

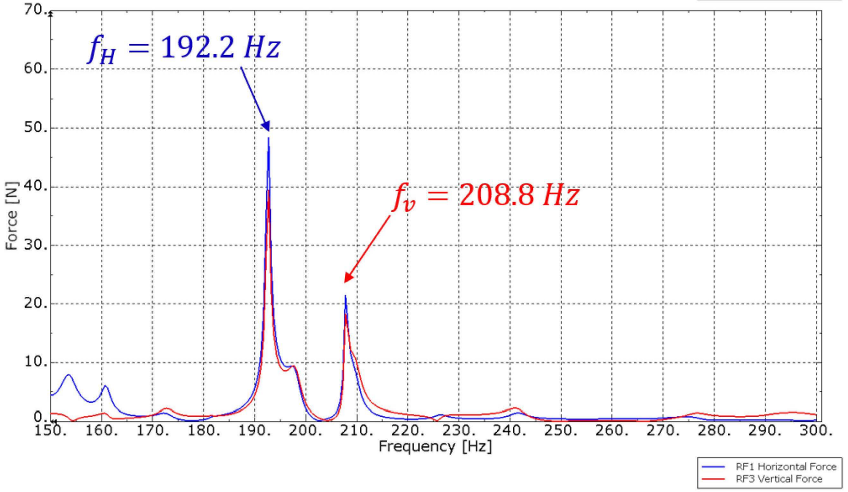

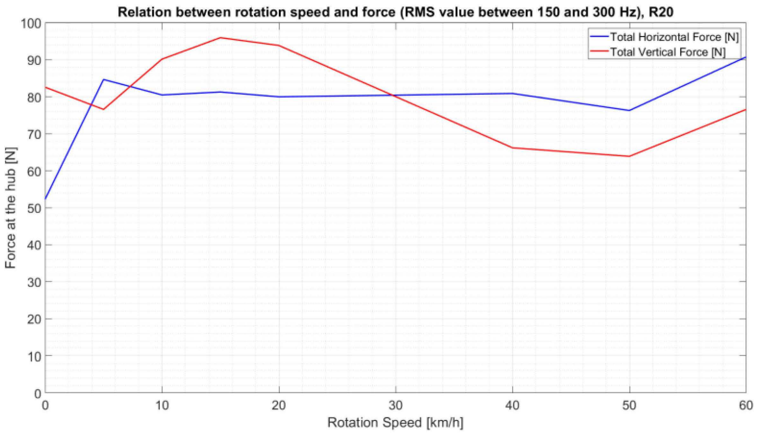

Conclusions

- FE simulations based on steady-state transport analysis were used to predict the acoustic mode frequency split for rolling tires
- Two candidate tires were investigated after first confirming the validity of the simulations through comparison of mobility and dispersion diagram with previously measured experimental results for the non-deformed case
- Both tires showed an increase in the frequency split as the rotation speed was increased, beginning at a speed of 20 km/h. Under 20 km/h, there was not a significant change in the frequency split.
- The force at the hub is observed to be a strong function of rotation speed, since it is affected by interaction of the split air-cavity modes and the split structural modes that result from rotation
- In the next stage of this work, hub force data measured in the laboratory for rolling tires will be quantitatively compared with the simulation results to demonstrate their reliability

Acknowledgement

- Ford Motor Company – Financial support / Tire & wheel sample provider
- Matthew Black – Main coordinator of this project
- Dan Haakenson – Technical advice and industrial feedback

THANK YOU

Won Hong Choi
choi124@purdue.edu
Ray W. Herrick Laboratories

J. Stuart Bolton
bolton@purdue.edu
Ray W. Herrick Laboratories

References

[1] Bernhard, R. and et al. (2012) “An Introduction to Tire/Pavement Noise of Asphalt Pavement, ” *Virginia Asphalt Association.*

[2] Sakata, T., Morimura, H. and Hideyuki, I. (1990) “ Effect of Tire Cavity Resonance on Vehicle Road Noise, ” *Tire Science and Technology*, Vol. **18(2)**, pp.68–79.

[3] Yamauchi, H. and Akiyoshi, Y. (2002) “ Theoretical Analysis of Tire Acoustic Cavity Noise and Proposal of Improvement Technique, ” *JSAE Review*, Vol. **23**, pp.89–94.

[4] Abaqus tutorial (2016), “ 3.1.9 Dynamic analysis of an air-filled tire with rolling transport effects , ”

[5] Yuting Liu, Xiandong Liu, and et al. (2018) “Research on mechanism and evolution features of frequency split phenomenon of tire acoustic cavity resonance,” Journal of Vibration and Control, Vol. **0(0)**, pp.1-13.

[6] Y.-J. Kim, J.S. Bolton (2004) “Effects of rotation on the dynamics of a circular cylindrical shell with application to tire vibration, ” Journal of Sound and Vibration, Vol. **275**, pp.605-621.